Synthesis of High Thermal Stability Polybenzoxazoles via *Ortho*-Imide-Functional Benzoxazine Monomers

Kan Zhang,[1,2] Jia Liu,[1] Seishi Ohashi,[1] Xiaoyun Liu,[2] Zhewen Han,[2] Hatsuo Ishida[1]

[1]Department of Macromolecular Science and Engineering, Case Western Reserve University, Cleveland, Ohio 44106
[2]School of Materials Science and Engineering, East China University of Science and Technology, Shanghai 200237, China
Correspondence to H. Ishida (E-mail: hxi3@cwru.edu)

Received 9 December 2014; accepted 21 January 2015; published online 00 Month 2015
DOI: 10.1002/pola.27565

ABSTRACT: We report our work for preparing cross-linked polyimide via a series of imide functional benzoxazine resins as precursors. The structures of synthesized monomers have been confirmed by ^{1}H NMR and FT-IR. Among this class of benzoxazine monomers, the *ortho*-imide functional benzoxazine resins show useful features both in the synthesis of benzoxazine monomers and the properties of the corresponding thermosets. For the cross-linked polyimides based on *ortho*-imide functional benzoxazine, an additional route is adopted to form a more thermally stable cross-linked polybenzoxazole with the release of carbon dioxide. The *ortho*-imide functional benzoxazine resins show the possibility to form high performance and even super high performance thermosets with low cost and easy processability. The thermal properties are evaluated by DSC and TGA. © 2015 Wiley Periodicals, Inc. J. Polym. Sci., Part A: Polym. Chem. **2015**, *00*, 000–000

KEYWORDS: benzoxazine; high temperature materials; polybenzoxazole; polyimides; thermosets

INTRODUCTION Aromatic polymer films have attracted much attention in the fields of microelectronics, aerospace and defense applications due to their excellent mechanical, thermal, and electrical properties and light weight.[1] Among these polymers, aromatic polyimides (PIs) possess high thermal stability, chemical resistance and good mechanical properties, which made them widely used as matrices of advanced composites.[2] The structure of the polyimide backbone determines the heat resistance as well as the chemical resistance. The rigidity, originating from the combination of the imide structure with an aromatic structure, results in polymers with a very high glass transition temperature (T_g). Moreover, the partial conjugation of the imide structure promotes a good oxidative stability.[3] However, the chemical structures that lead PIs to very high thermal stability also cause processing difficulties. Therefore, the trade-off generally exists between the thermal resistance and processability.[4] More recently, the concept of crosslinking PIs has become popular.[5]

While several articles on polyimide/benzoxazine resin blend have been reported,[6–9] PIs with benzoxazine in the same molecule have rarely been reported.[10,11] Benzoxazine can be synthesized by Mannich condensation from phenol, amine, and formaldehyde.[12,13] The major advantages of polybenzoxazine include good mechanical and thermal properties, low water absorption, high carbon residue, and low surface energy.[14–21] The most interesting and unique characteristic of this class of polymers is their extraordinarily rich molecular design flexibility that allows designing a variety of molecular structures to tailor the desired properties.

Polybenzoxazoles (PBOs) are a class of high-performance polymers used to manufacture organic fiber for ballistic applications based on their very high strength, modulus, and thermal stability.[22,23] While the very high rigidity of PBO molecules is responsible for the outstanding performance, it also leads to difficulties in synthesis and fabrication. The major drawback of the rigid structure is the insolubility of the PBO in organic solvents as well as the lack of melting phenomenon without thermal degradation, which hinders the fabrication of PBO into films and fibers. Poly(phosphoric acid) is one of very few solvents that can be used for PBO synthesis. However, the use of this solvent leads to a known aging problem at moderately elevated temperature under humid environment through the hydrolysis reaction of the oxazole rings which is catalyzed by the acid residues.[24,25] Therefore, developing a new approach for synthesizing PBO without the use of poly(phosphoric acid) as solvent is of strong interest.[18,26]

We reported two *para*-imide functional benzoxazine monomers in our previous article.[27] However, the imide-functional benzoxazines were just the intermediate for the preparation of amino-functional benzoxazine, and the synthesis and understanding of the function of the imide-containing

benzoxazine as a precursor for benzoxazole was not intended. We used tetrachlorophthalimide to protect the amino group, followed by deprotection to obtain primary amine-functional benzoxazine. However, in the current study, a series of aromatic functional imide containing benzoxazine monomers were prepared. One of particular interest is the ability for the *ortho*-imide functional benzoxazines to be the precursor for further structural transformation to polybenzoxazoles. Additionally, the *ortho*-imide functional benzoxazine shows great advantages in the synthesis of benzoxazine monomers compared with the *para*-imide functional benzoxazine from the view points of shorter reaction time, higher yield, and ease of purification. Thus, the subsequent *in situ* thermal conversion of the *ortho*-imide functional polybenzoxazines into polybenzoxazole (PBO) could provide a low-cost, easy processing, and environmentally friendly alternative method for preparing PBO films, fibers and composites.

This polybenzoxazine derived from *ortho*-functional benzoxazine monomer was a subject of very recent article where unexpected superior properties were observed for *ortho*-functional benzoxazine to its *para*-counterpart.[28] This *ortho* to *para* relationship observed on polybenzoxazine is totally opposite from the literature examples of many well-known polymers. The current article attempts to combine these superior properties of the *ortho*-functional benzoxazines to *para*-functional benzoxazines with the smart chemistry of structure transformation from polybenzoxazine to polybenzoxazole during the elevated thermal treatment.

EXPERIMENTAL

Materials

o-Aminophenol, *p*-aminophenol, phthalic anhydride, and paraformaldehyde (99%), were used as received from Sigma-Aldrich. 4,4'-Diaminodiphenylmethane (DDM) (98%), was purchased from Aldrich. Aniline was purchased from Aldrich and purified by distillation. Acetic acid, methanol, xylenes, and sodium sulfate were obtained from Fisher Scientific and used as received.

Characterization

^{1}H nuclear magnetic resonance (NMR) spectra were recorded on a Varian Oxford AS300 at a proton frequency of 300 MHz. The average number of transients for ^{1}H NMR measurement was 64. A relaxation time of 10 s was used for the integrated intensity determination of ^{1}H NMR spectra. Fourier transform infrared (FT-IR) spectra were measured by a Bomem Michelson MB100 FT-IR spectrometer, which was connected with a dry air purge unit and a deuterated triglycine sulfate (DTGS) detector. Sixty four scans were coadded to obtain a spectrum at a resolution of 4 cm^{-1}. All samples were finely ground with KBr powder and pressed into disk and the spectrum was taken as the transmission mode. A TA Instruments DSC model 2920 was used with a heating rate of 10 °C/min and a nitrogen flow rate of 60 mL/min for all tests of differential scanning calorimetric (DSC) study. All samples were sealed in hermetic aluminum pans with lids. Thermogravimetric analyses (TGA) were performed on a TA Instruments High Resolution 2950 Thermogravimetric Analyzer that was purged with nitrogen at a flow rate of 40 mL/min. A heating rate of 10 °C/min was used.

Preparation of 2-(4-Hydroxyphenyl)-Isoindoline-1,3-Dione (p-PP)

Into a 250 mL round flask were placed phthalic anhydride (7.41 g, 0.05 mol), *p*-aminophenol (5.41 g, 0.05 mol), and 60 mL of acetic acid. The mixture was stirred and refluxed for 6 h. After cooling to room temperature, the precipitate was filtered and washed with 200 mL of methanol. Removal of solvent by evaporation afforded a white powder (yield ca. 86%).

^{1}H NMR (DMSO), ppm: $\delta = 6.82–7.93$ (8H, Ar), 9.76 (OH). IR spectra (KBr, cm^{-1}) = 3412 (O—H stretching), 1786, 1713 (Imide I), 1398 (imide II,C—N stretching), 722 (C═O bending).

Preparation of 2-(2-Hydroxyphenyl)-Isoindoline-1, 3-Dione (o-PP)

Into a 250 mL round flask were placed phthalic anhydride (7.41 g, 005 mol), *o*-aminophenol (5.41 g, 0.05 mol), and 60 mL of acetic acid. The mixture was stirred and refluxed for 6 h. After cooling to room temperature, the precipitate was filtered and washed with 200 mL of methanol. Removal of solvent by evaporation afforded an orange crystal (yield ca. 90%).

^{1}H NMR (DMSO), ppm: $\delta = 6.82–7.93$ (8H, Ar), 9.76 (OH). IR spectra (KBr, cm^{-1}) = 3383 (O—H stretching), 1787, 1700 (Imide I), 1390 (imide II, C—N stretching), 722 (C═O bending).

Preparation of 2-(3-Phenyl-3,4-Dihydro-2H-benzo[e][1,3] oxazin-6-yl)-isoindoline-1,3-dione (pPP-a)

Into a 100 mL round flask were added 30 mL of mixed isomer xylenes, aniline (1.40 g, 0.015 mol), *p*-PP (3.59 g, 0.015 mol), and excess of paraformaldehyde (1.80 g, 0.06 mol). The mixture was stirred at 120 °C for 48 h. The mixture was cooled to room temperature and filtered off. Then the solution was precipitated into 100 mL of methanol. Removal of solvent by filtering afforded a brown powder. (yield ca. 57%).

^{1}H NMR (DMSO), ppm: $\delta = 4.71$ (s, Ar—CH_2—N, oxazine), 5.50 (s, O—CH_2—N, oxazine), 6.84–7.96 (12H, Ar). IR spectra (KBr), cm^{-1}: 1773, 1720 (imide I), 1497 (stretching of trisubstituted benzene ring), 1383 (imide II), 1235 (C—O—C asymmetric stretching), 1194 (C—N—C asymmetric stretching), 945 (out-of-plane C—H).

Preparation of 2-(3-Phenyl-3,4-dihydro-2H-benzo[e][1,3] oxazin-8-yl)-isoindoline-1,3-dione (oPP-a)

Into a 100 mL round flask were added 30 mL of xylenes, aniline (1.40 g, 0.15mol), *o*-PP (3.59 g, 0.015mol), and paraformaldehyde (0.91g, 0.03 mol). The mixture was stirred at 120 °C for 6 h. The mixture was cooled to room temperature and precipitated into 100 mL of methanol. Removal of solvent by filtering afforded a yellow powder. (yield ca. 95%, m.p. 209 °C).

^{1}H NMR (DMSO), ppm: $\delta = 4.72$ (s, Ar—CH_2—N, oxazine), 5.42 (s, O—CH_2—N, oxazine), 6.85–7.96 (12H, Ar). IR spectra (KBr), cm^{-1}: 1774, 1719 (imide I), 1497 (stretching of trisubstituted benzene ring), 1385 (imide II), 1231 (C—O—C asymmetric stretching), 1179 (C—N—C asymmetric stretching), 924 (out-of-plane C—H).

Preparation of 2,2'-(3,3'(4,4'-Methylenebis (4,1-phenylene))-bis(3,4-dihydro-2H-benzo[e][1,3] oxazin-6,3-diyl))-bis(isoindoline-1,3-dione) (pPP-ddm)

Into a 100 mL round flask were added 30 mL of xylenes, DDM (1.49 g, 0.0075 mol), *p*-PP (3.59 g, 0.015 mol), and paraformaldehyde (0.91 g, 0.03 mol). The mixture was stirred at 120 °C for 36 h. The mixture was cooled to room temperature and filtered off. Then the solution was precipitated into 100 mL of methanol. Removal of solvent by filtering afforded a yellow powder. (yield ca. 50%).

^{1}H NMR (DMSO), ppm: $\delta = 3.71$ (s, CH_2), 4.65 (s, Ar—CH_2—N, oxazine), 5.44 (s, O—CH_2—N, oxazine), 6.80–7.92 (8H, Ar). IR spectra (KBr), cm^{-1}: 1773, 1720 (imide I), 1499 (stretching of trisubstituted benzene ring), 1381 (imide II), 1236 (C—O—C asymmetric stretching), 1185 (C—N—C asymmetric stretching), 944 (out-of-plane C—H).

Preparation of 2,2'-(3,3'(4,4'-Methylenebis (4,1-phenylene))-bis(3,4-dihydro-2H-benzo[e][1,3] oxazin-8,3-diyl))-bis(isoindoline-1,3-dione) (oPP-ddm)

Into a 100 mL round flask were added 20 mL of xylenes, DDM (1.49 g, 0.0075 mol), *o*-PP (3.59 g, 0.015 mol), and paraformaldehyde (0.91 g, 0.03 mol). The mixture was stirred at 120 °C for 6 h. The mixture was cooled to room temperature and precipitated into 100 mL of methanol. Removal of solvent by filtering afforded a yellow powder. (yield ca. 93%, m.p. 225 °C).

^{1}H NMR (DMSO), ppm: $\delta = 3.71$ (s, CH_2), 4.63 (s, Ar—CH_2—N, oxazine), 5.35 (s, O—CH_2—N, oxazine), 6.94–7.96 (8H, Ar). IR spectra (KBr), cm^{-1}: 1780, 1723 (imide I), 1485 (stretching of trisubstituted benzene ring), 1383 (imide II), 1230 (C—O—C asymmetric stretching), 1179 (C—N—C asymmetric stretching), 925 (out-of-plane C—H).

Polymerization of Imide Functional Benzoxazines

A solution of 30% solid content of the monomers in DMF was prepared. Then, the solution was cast over a dichlorodimethylsilane-pretreated glass plate. The film was dried in an air circulating oven at 100 °C for 24h to remove the solvent completely. The film as fixed on a glass plate was polymerized stepwise at 120, 140, 160, 200, 230 °C for 1 h each, and then slowly cooled to room temperature. They showed dark brown color with thickness ranging from 0.1 to 0.3 mm.

RESULTS AND DISCUSSION

Preparation of Imide Functional Benzoxazine Monomers

A successful synthesis of imide monofunctional and difunctional benzoxazine monomers has been achieved using primary amine (aniline and DDM), formaldehyde, and imide functional phenol (*ortho*- and *para*-isomers) as shown in Scheme 1.

Prior to this study, we also attempted to prepare imide functional diphenol using diphthalic anhydride and bis(phthalic anhydride) with aminophenol. However, it was difficult to obtain the purified benzoxazine monomers due to the poor solubility of imide functional diphenol in ordinary solvents.

To overcome the above problem, we chose phthalic anhydride to prepare imide functional monophenols (*p*-phenol phthalamide and *o*-phenol phthalamide, hereinafter abbreviated as *p*-PP and *o*-PP) as the first step, and then *p*-PP and *o*-PP were reacted with amine and paraformaldehyde to prepare the imide monofunctional and difunctional benzoxazine monomers. At the second step, the synthesis method and the reaction time of *para*-imide functional benzoxazine monomers (*p*PP-a and *p*PP-ddm) exhibited great differences from *ortho*-isomers (*o*PP-a and *o*PP-ddm). The synthesis of *p*PP-a required excess paraformaldehyde and the reaction time was as long as 48 h. In the case for preparing *p*PP-ddm, a considerable amount of gel formation was observed during the early stage of the synthesis. This insoluble gel did not disappear despite applying long reaction time, leading to poor yield. However, both the syntheses of *o*PP-a and *o*PP-ddm completed in just 6 h, which led to a transparent solution. One possibility is that the intramolecular hydrogen bond between the phenolic OH group and one of the carbonyl group decreases the polarity of *o*-PP, which improves the solubility of *o*-PP in aprotic solvent. At the same time, the intramolecular hydrogen bond also accelerates the ionization of phenolic OH group during the initial stage for forming benzoxazine ring. As a result, the ring-closing process of benzoxazine for *ortho*-isomers becomes much easier than *para*-isomers.

The structures of the monomers were confirmed using ^{1}H NMR spectra, as depicted in Figures 1 and 2. The characteristic resonances attributed to the benzoxazine structure, Ar—CH_2—N— and —O—CH_2—N— for *p*PP-a, *p*PP-ddm, *o*PP-a, *o*PP-ddm are observed at 4.71, 5.50; 4.65, 5.44; 4.72, 5.42; 4.63, 5.35 ppm, respectively. Also the ^{1}H NMR spectra confirm the presence of methylene group (—CH_2—) at 3.71 ppm for both *p*PP-ddm and *o*PP-ddm. Besides, the ^{1}H NMR end-group analysis indicates the purity of *p*PP-a, *p*PP-ddm, *o*PP-a and *o*PP-ddm to be 97.9%, 97.0%, 99.5%, and 98.2%, respectively.

There are a number of infrared absorption bands, highlighted in Figure 3, that are used to verify the formation of oxazine rings in each monomer. For example, the characteristic doublet at 1780 to 1773 cm^{-1} and 1723 to 1719 cm^{-1} are the typical bands for imide, which are attributed to the imide C—C(=O)—C antisymmetric and symmetric stretching, respectively.[29] In addition to these bands, the presence of imide is seen by the other characteristic bands at 1385 to 1381 cm^{-1} which is due to the axial stretching of C—N bonding.[30,31] The bands characteristic of antisymmetric

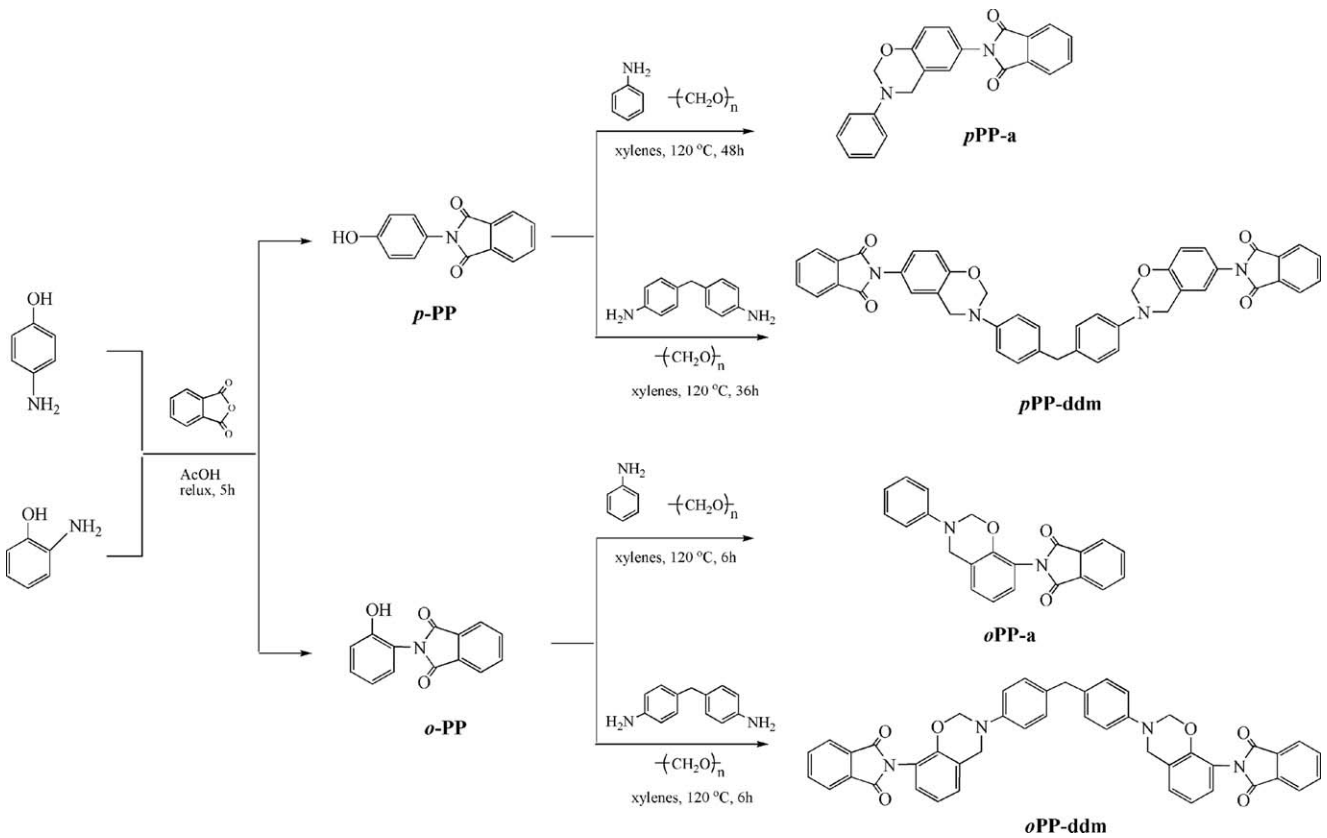

SCHEME 1 Preparation of imide-functional benzoxazine monomers.

trisubstituted benzene that appear between 1499 and 1485 cm^{-1} confirm the incorporation of imide group into benzoxazine monomers. Besides, the presence of the benzoxazine ring aromatic ether in the monomers is indicated by the band centered in the range of 1236 to 1230 cm^{-1} due to the C—O—C antisymmetric stretching modes.[32] Finally, the characteristic out-of-plane absorption modes of benzene with an attached oxazine ring are located at 945, 944, 924, 925 cm^{-1} for *p*PP-a, *p*PP-ddm, *o*PP-a, and *o*PP-ddm, respectively.[33]

Polymerization Behavior of Benzoxazine Monomers

The polymerization profile of imide functional benzoxazine monomers was studied by DSC as depicted in Figures 4 and

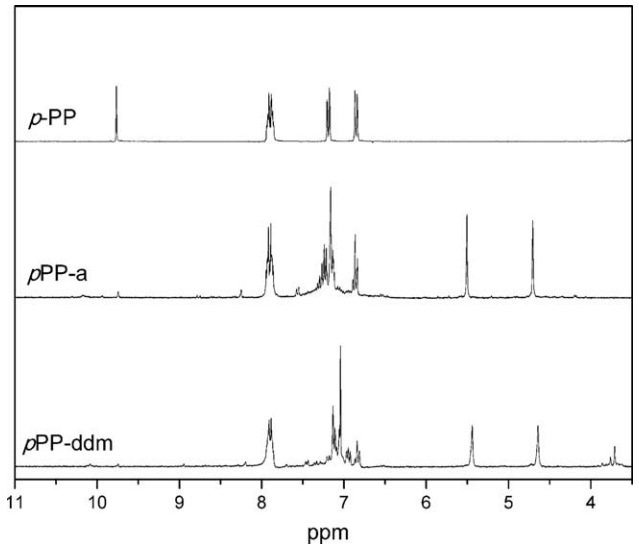

FIGURE 1 ^{1}H NMR spectra of *p*-PP, *p*PP-a, and *p*PP-ddm.

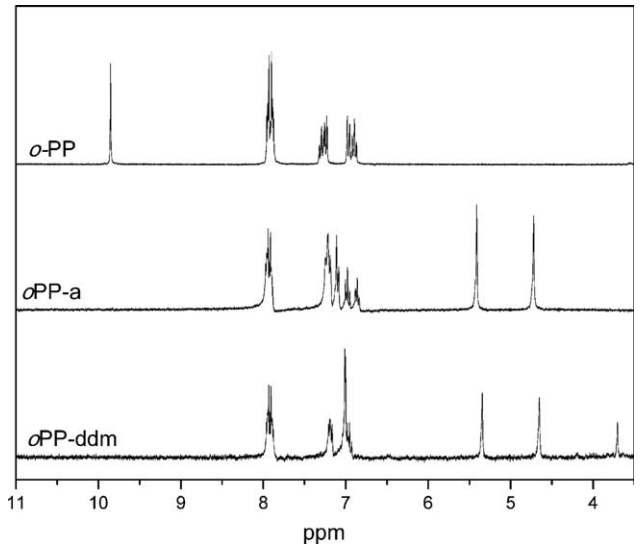

FIGURE 2 ^{1}H NMR spectra of *o*-PP, *o*PP-a, and *o*PP-ddm.

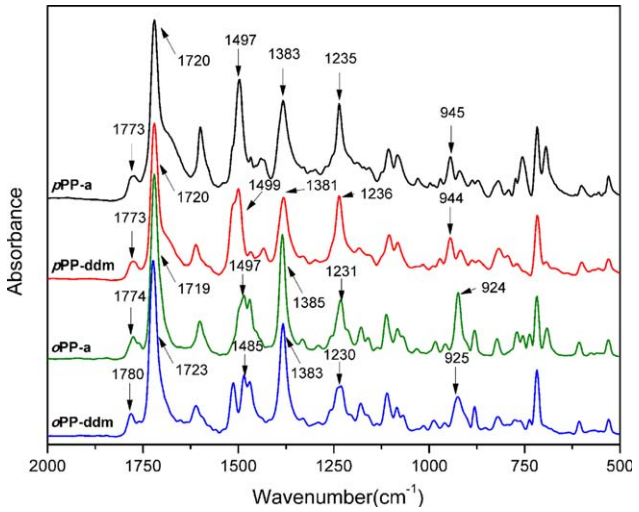

FIGURE 3 FT-IR spectra of benzoxazine monomers. [Color figure can be viewed in the online issue, which is available at wileyonlinelibrary.com.]

5 and the results are summarized in Table 1. The thermograms show that the maxima of the ring-opening polymerization of monofunctional benzoxazine monomers of *p*PP-a and *o*PP-a centered at 225 and 234 °C, respectively. However, the maximum of polymerization is shifted for the difunctional benzoxazine monomers of *p*PP-ddm and *o*PP-ddm to 241 and 243 °C, respectively. Moreover, the *ortho*-benzoxazine monomers, *o*PP-a and *o*PP-ddm, show lower values of the heat of polymerization compared to the *para*-isomers, *p*PP-a and *p*PP-ddm. For example, the heat of polymerization are 214 and 185 J/g for *o*PP-a and *o*PP-ddm, respectively. However, *p*PP-a and *p*PP-ddm exhibit higher heat of polymerization of 225 and 233 J/g, respectively. The values of the lower heat of polymerization for the *ortho*-functional monomers are possibly due to the endotherm of melting which is partially overlapped with the polymerization exotherm.

TABLE 1 DSC Thermograms of Benzoxazine Monomers

Monomer	Onset Temp (°C)	Max Temp (°C)	Heat of Polymerization (J/g)
*p*PP-a	170	225	225
*p*PP-ddm	181	241	233
*o*PP-a	213	234	214
*o*PP-ddm	221	243	185

Thermal Properties of Thermosets Derived from Imide-Functional Benzoxazine Monomers

Figure 6 shows the DSC thermograms of the heat-treated mono- and difunctional monomeric benzoxazines with the heating schedule stated in the experimental section. For the polybenzoxazines based on monofunctional benzoxazine monomers, the T_g are lower than the polybenzoxazines of difunctional benzoxazine monomers, which are due to the low cross-linking density of mono-functional benzoxazines despite some expected reactivity on the aromatic ring of the aniline moiety. Many monofunctional benzoxazines show small linear or branched oligomers due to the competing terminating effect of intramolecular hydrogen bonding of the active species[34] and only a few exceptional monofunctional benzoxazines cross-link. For the imide functional polybenzoxazines based on difunctional monomers, both of them show the T_g as high as over 200 °C. The thermal properties are summarized in Table 2. While these T_gs are relatively high, it is nonetheless lower value in comparison to typical polyimide. This is because the imide moiety was incorporated at a chain end rather than part of the main chain to achieve a balance of improving thermal property and maintaining the solubility and processability.

The thermal stability of polybenzoxazines has been studied by TGA (Fig. 7). It is well-established that the polymerization of benzoxazines occurs through oxazine ring-opening without producing any byproduct. The polybenzoxazines of *para*-

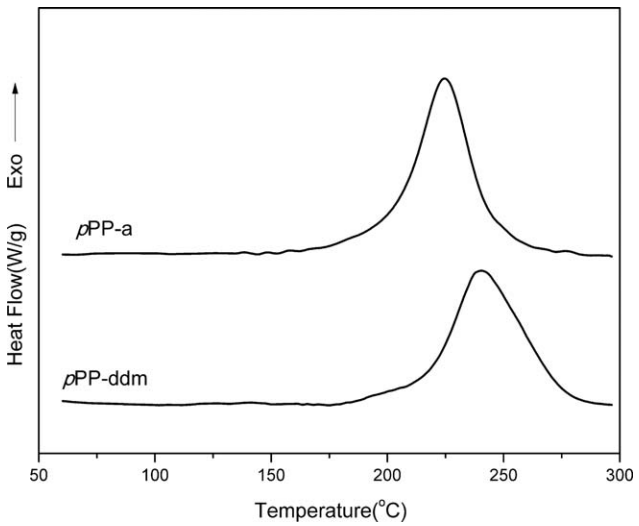

FIGURE 4 DSC thermograms of *para*-benzoxazine monomers *p*PP-a and *p*PP-ddm.

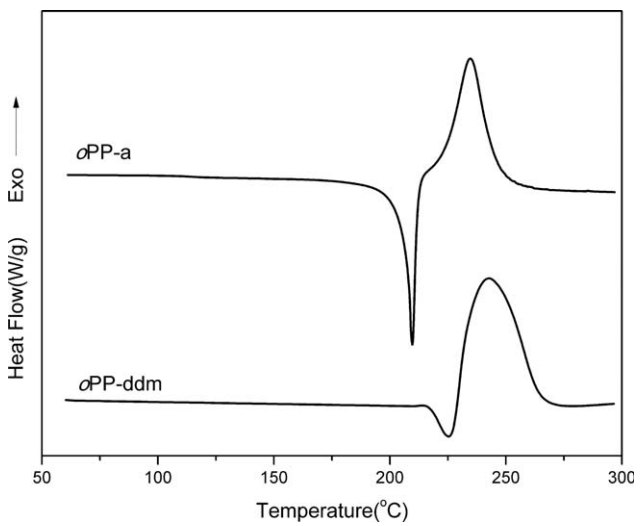

FIGURE 5 DSC thermograms of *ortho*-benzoxazine monomers *o*PP-a and *o*PP-ddm.

TABLE 2 Thermal Properties of Imide Functional Polybenzoxazines

Polybenzoxazine Based On	T_g/DSC (°C)	T_5 (°C)	T_{10} (°C)	Y_c (wt %)
*p*PP-a	162	289	318	39
*p*PP-ddm	204	343	384	53
*o*PP-a	163	319	358	60
*o*PP-ddm	201	303	354	58

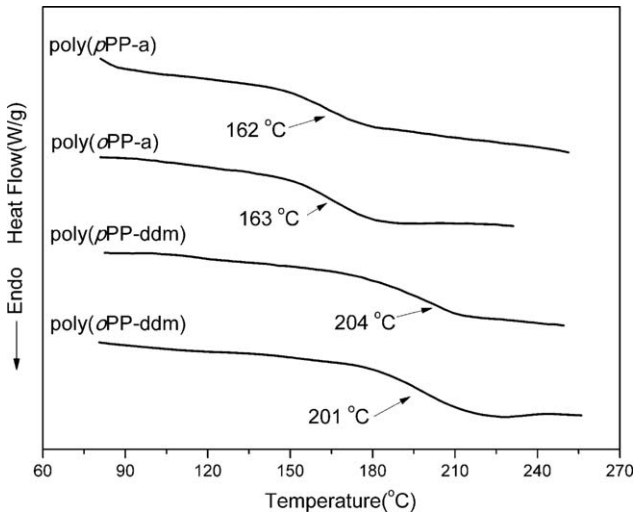

FIGURE 6 DSC thermograms of polybenzoxazines recorded under nitrogen at a heating of 10 °C/min.

functional isomers (*p*PP-a and *p*PP-ddm) show degradation similar to typical polybenzoxazines. However, the polybenzoxazines of *ortho*-funtional isomers (*o*PP-a and *o*PP-ddm) show different degradation profiles. The derivative weight loss curves are also shown in Figure 7. From the comparison of four polybenzoxazines, we observe that both poly(*p*PP-a)

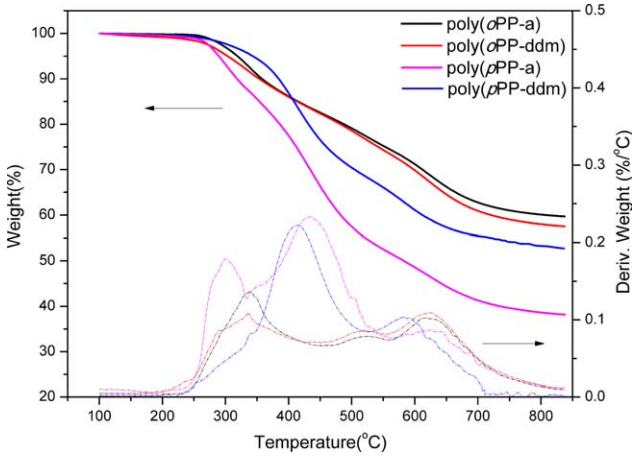

FIGURE 7 Thermogravimetric analysis of imide-functional polybenzoxazines. [Color figure can be viewed in the online issue, which is available at wileyonlinelibrary.com.]

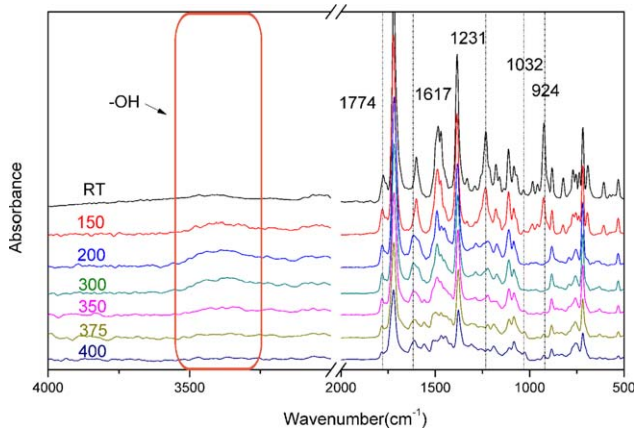

FIGURE 8 FT-IR spectra of *o*PP-a after various thermal treatment. [Color figure can be viewed in the online issue, which is available at wileyonlinelibrary.com.]

and poly(*p*PP-ddm) show a high weight-loss stage in the range of 350 to 550 °C. On the contrary, the poly(*o*PP-a) and poly(*o*PP-ddm) show the stable weight loss rates in this temperature range. As a result, the char yields of the polybenzoxazines based on *ortho*-monomers are much higher than the polybenzoxazines based on *para*-isomers. The thermal properties data are also summarized in Table 2.

Moreover, the TGA results suggest that within 350 to 550 °C, special thermal events are taking place to poly(*o*PP-a) and poly(*o*PP-ddm). Mathias and others reported the possible thermal conversion of *ortho*-hydroxypolyimides into polybenzoxazoles with loss of carbon dioxide at temperature around 400 °C,[35–39] although this mechanism was later questioned by Hodgkin and Dao in 2009.[40] Somewhat different structure from the current article but is still along the similar approach of thermally induced structural transformation into more thermally stable benzoxazole structure, is the series of

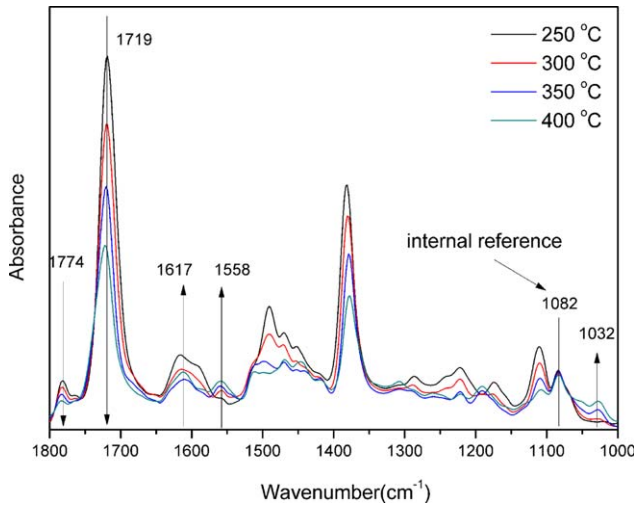

FIGURE 9 Normalized FT-IR spectra of *o*PP-a by the internal reference at 1082 cm^{-1}. [Color figure can be viewed in the online issue, which is available at wileyonlinelibrary.com.]

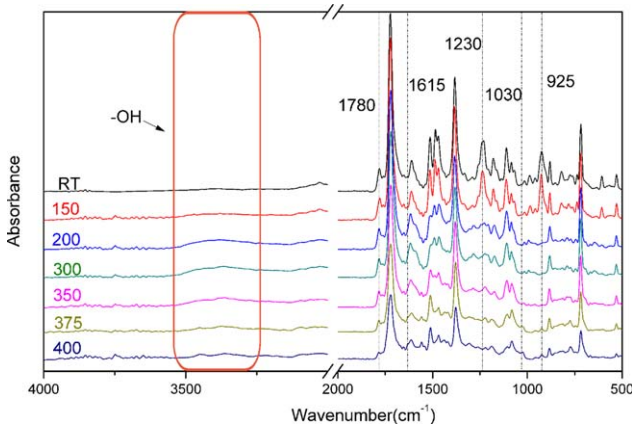

FIGURE 10 FT-IR spectra of *o*PP-ddm after various thermal treatment. [Color figure can be viewed in the online issue, which is available at wileyonlinelibrary.com.]

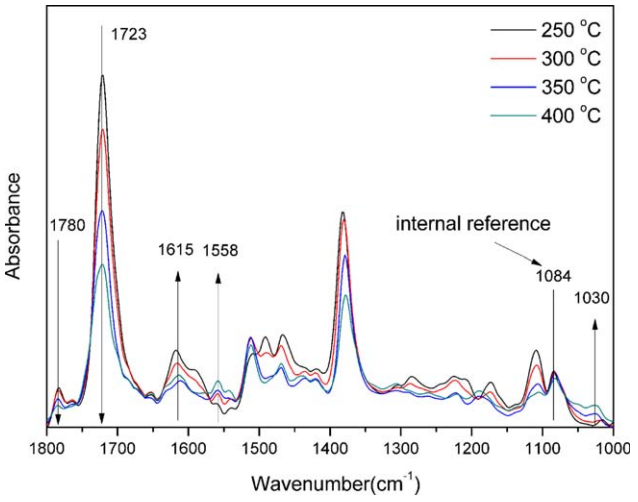

FIGURE 11 Normalized FT-IR spectra of *o*PP-ddm by the internal reference at 1084 cm^{-1}. [Color figure can be viewed in the online issue, which is available at wileyonlinelibrary.com.]

investigation of Khanna et al. on the degradation mechanism of para-aromatic amide and its chlorinated analogues where the chlorine atom is placed at the ortho position to the amide group.[41–43] In order to qualitatively study the structure evolution, FT-IR analyses were carried out and the spectra for poly(*o*PP-a) are displayed in Figures 8 and 9. As shown in Figure 8, the characteristic absorption bands at 1231 cm^{-1} (C—O—C asymmetric stretching modes) and 924 cm^{-1} (the out-of-plane bending vibration of C—H) gradually disappear from room temperature to 200 °C. Meanwhile, the broad band of —OH around 3400 cm^{-1} gradually appears, reflecting the ring-opening of the benzoxazine. However, with the further increasing the temperature, the —OH band gradually disappears from 300 to 400 °C. This result is consistent with the possible thermal conversion of *ortho*-hydroxypolyimides into polybenzoxazoles. If this explanation is valid, the intensity of imide group should also decrease while the intensity of benzoxazole group should increase with respect to the internal reference. This explanation is well supported by the fact that the characteristic bands for imide at 1774 and 1719 cm^{-1} decrease, and two new peaks appear at 1558 and 1032 cm^{-1} as shown in Figure 9. The C═N stretching in benzoxazole can also be found at 1617 cm^{-1}. The peak at 1558 cm^{-1} is the typical absorption band of benzoxazole and 1032 cm^{-1} is due to the —O—C stretching of benzoxazole group.[44,45] We did not apply

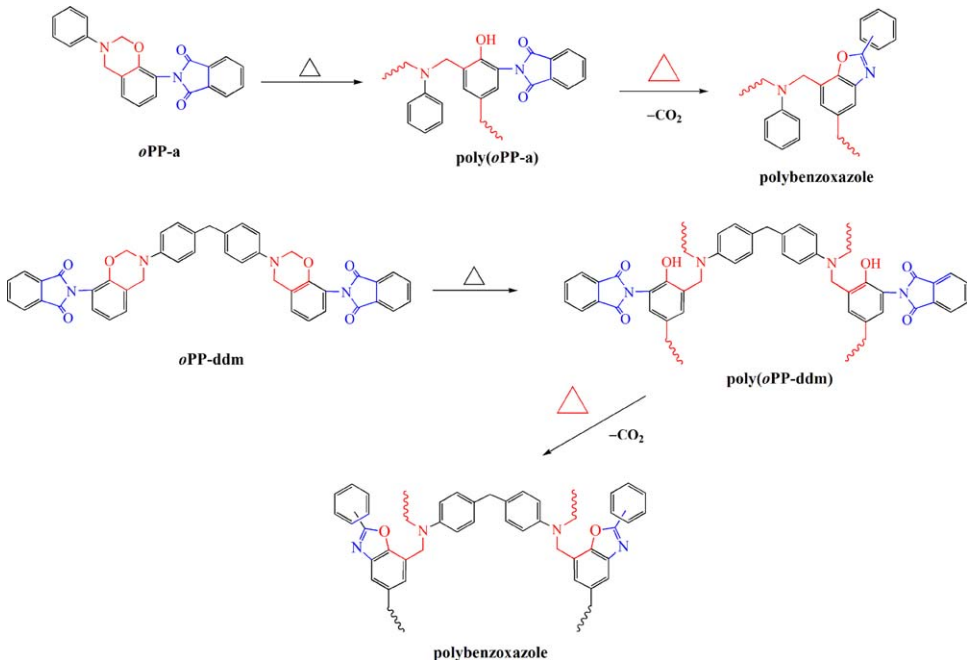

SCHEME 2 Thermal behavior of *ortho*-functional benzoxazine monomers *o*PP-a and *o*PP-ddm. [Color figure can be viewed in the online issue, which is available at wileyonlinelibrary.com.]

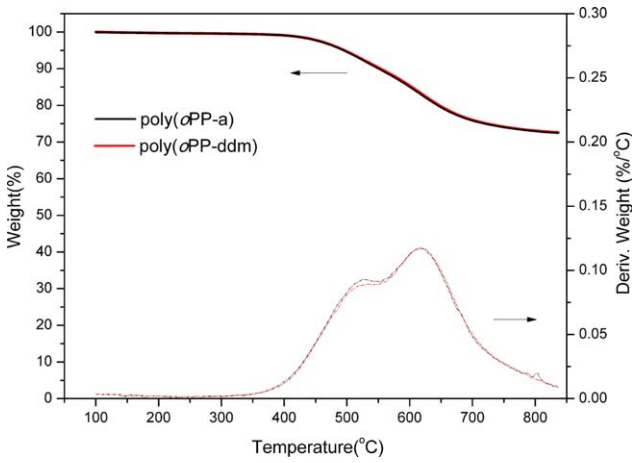

FIGURE 12 Thermogravimetric analysis of poly(*o*PP-a) and poly(*o*PP-ddm) after thermal treatment at 400 °C. [Color figure can be viewed in the online issue, which is available at wileyonlinelibrary.com.]

further thermal treatment over 400 °C to complete the conversion in order to avoid the degradation of the cross-linked segments of polybenzoxazine after 400 °C.

For poly(*o*PP-ddm), similar phenomenon can be observed in Figures 10 and 11. As a result, the thermal behavior of *o*PP-a and *o*PP-ddm can be described as Scheme 2.

In order to further confirm the occurrence of benzoxazole cyclization, poly(*o*PP-a) and poly(*o*PP-ddm) were further treated at 400 °C for 1 h, the TGA thermograms of these polymers are shown in Figure 12. After the thermal treatment, the profiles of them are nearly the same, which suggests both *ortho*-compounds follow the same degradation mechanism. Besides, their maxima of weight-loss rates are as high as 618 °C, and the char yield is as high as 73%, which suggest extremely high thermal stability of both cross-linked polybenzoxazoles with $T_{d5} = 505$ °C.

CONCLUSIONS

A new class of imide functional benzoxazine monomers has been successfully synthesized. Among these new benzoxazine monomers, *ortho*-imide functional benzoxazine resins show advantages both in the synthesis of benzoxazine monomers and the properties of the corresponding thermosets compared with *para*-imide functional benzoxazine resins. Besides, the cross-linked polyimides based on *ortho*-imide functional benzoxazine can be adopted to form a more thermally stable cross-linked polybenzoxazole. This research suggests the possibility to form high performance thermosets with low molecular weight compound.

ACKNOWLEDGMENTS

The author (K. Zhang) is indebted to the partial support of Chinese Scholarship Council (CSC) Program.

REFERENCES AND NOTES

1 M. A. Meador, *Annu. Rev. Mater. Sci.* **1988**, *28*, 599–630.

2 P. Vandezande, L. E. M. Gevers, I. F. J. Vankelecom, *Chem. Soc. Rev.* **2008**, *37*, 365–405.

3 J. Kirby, Polyimide: Materials Processing and Applications; Pergamon Press: Oxford, **1992**; Vol. 5, pp 158.

4 P. E. Cassidy, N. C. Fawcett, In Encyclopedia of Polymer Science and Technology; H. F. Mark, A. Standen, Eds.; Wiley: New York, **1979**; Vol. 118, pp704–719.

5 K. Vanherch, G. Koeckelberghs, I. F. J. Vankelecom, *Prog. Polym. Sci.* **2013**, *38*, 874–896.

6 T. Takeichi, Y. Guo, S. Rimdusit, *Polymer* **2005**, *46*, 4909–4916.

7 T. Takeichi, T. Agag, R. Zeidam, *J. Polym. Sci. Part A: Polym. Chem.* **2001**, *39*, 2633–2641.

8 S. Tiptipakorn, S. Damrongsakkul, S. Ando, K. Hemvichian, S. Rimdusit, *Polym. Degrad. Stab.* **2007**, *92*, 1265–1278.

9 P. Zhao, X. M. Chen, Q. C. Ran, Y. Gu, *J. Appl. Polym. Sci.* **2013**, *128*, 2865–2874.

10 M. W. Wang, C. H. Lin, T. Y. Juang, *Macromolecules* **2013**, *46*, 8853–8863.

11 K. C. Chen, H. T. Li, W. B. Chen, C. H. Liao, K. W. Sun, F. C. Chang, *Polym. Intern.* **2011**, *60*, 432–442.

12 F. Holly, A. C. Cope, *J. Am. Chem. Soc.* **1944**, *66*, 1875–1879.

13 X. Ning, H. Ishida, *J. Polym. Sci. Part A: Polym. Chem.* **1994**, *32*, 1121–1129.

14 T. Endo, A. Sudo, *J. Polym. Sci. Part A: Polym. Chem.* **2009**, *47*, 2847–2858.

15 Y. Cheng, J. Yang, Y. Jin, D. Deng, F. Xiao, *Macromolecules* **2012**, *45*, 4085–4091.

16 B. Kiskan, B. Aydogan, Y. Yagci, *J. Polym. Sci. Part A: Polym. Chem.* **2009**, *47*, 804–811.

17 P. V. Herreta, H. Ishida, *J. Polym. Sci. Part A: Polym. Chem.* **2009**, *47*, 5871–5881.

18 T. Agag, J. Liu, R. Graf, H. W. Spiess, H. Ishida, *Macromolecules* **2012**, *45*, 8991–8997.

19 K. Zhang, Q. X. Zhuang, Y. C. Zhou, X. Y. Liu, G. Yang, Z. W. Han, *J. Polym. Sci. Part A: Polym. Chem.* **2012**, *50*, 5115–5123.

20 Y. Yagci, B. Kiskan, N. N. Ghosh, *J. Polym. Sci. Part A: Polym. Chem.* **2008**, *47*, 5565–5576.

21 M. Spontón, M. S. Larrechi, J. C. Ronda, M. Galià, V. Cádiz, *J. Polym. Sci. Part A: Polym. Chem.* **2008**, *46*, 7162–7172.

22 J. F. Wolfe, F. E. Arnold, *Macromolecules* **1981**, *14*, 909–915.

23 J. F. Wolfe, B. H. Loo, F. E. Arnold, *Macromolecules* **1981**, *14*, 915–920.

24 T. Kitagawa, H. Murase, K. Yabuki, *J. Polym. Sci. Part B: Polym. Phys.* **1998**, *36*, 39–48.

25 T. Kitagawa, K. Yabuki K., *J. Appl. Polym. Sci.* **2001**, *80*, 1030–1036.

26 T. Fukumaru, Y. Seagusa, T. Fujigaya, N. Nakashima, *Macromolecules* **2014**, *47*, 2088–2095.

27 T. Agag, C. R. Arza, F. H. J. Mauer, H. Ishida, *Macromolecules* **2010**, *43*, 2748–2758.

28 J. Liu, H. Ishida, *Macromolecules*, **2014**, *47*, 5682–5690.

29 K. P. Pramoda, S. L. Liu, T. S. Chung, *Macromol. Mater. Eng.* **2002**, *287*, 931–937.

30 H. Ishida, S. T. Wellinghoff, E. Baer, J. L. Koenig, *Macromolecules* **1980**, *13*, 826–834.

31 B. T. Low, Y. Xiao, T. S. Chung, Y. Liu, *Macromolecules* **2008**, *41*, 1297–1309.

32 T. Agag, T. Takeichi, *Macromolecules* **2003**, *36*, 6010–1017.

33 J. Dunkers, H. Ishida, *Spectrochim. Acta.* **1995**, *51*, 1061–1074.

34 K. Hemvichian, H. Ishida, *Polymer* **2002**, *43*, 4391–4402.

35 G. L. Tullos, J. M. Powers, S. J. Jeskey, L. J. Mathias, *Macromolecules* **1999**, *11*, 3598–3612.

36 T. Okabe, T, A. Morikawa, *High Perform. Polym.* **2008**, *20*, 53–66.

37 H. B. Park, C. H. Jung, Y. M. Lee, A. J. Hill, S. J. Pas, S. T. Mudie, E. V. Wagner, B. D. Freeman, D . J. Cookson, *Science* **2007**, *318*, 254–258.

38 E. Schab-Balcexak, M. Jikei, M. Kaminoto, *Polym. J.* **2003**, *35*, 208–212.

39 D. Guzman-Lucero, D. Likhatcher, *Polym. Bull.* **2002**, *48*, 261–269.

40 J. H. Hodgkin, B. N. Dao, *Eur. Polym. J.* **2009**, *45*, 3081–3092.

41 Y. P. Khanna, E. M. Pearce, J. S. Smith, D. T. Burkitt, H. Njuguna, D. M. Hindenlang, B. D. Forman, *J. Polym. Sci. Part A: Polym. Chem.* **1981**, *19*, 2817–2834.

42 C. Karydas, W. T. Whang, E. M. Pearce, *J. Polym. Sci. Part A: Polym. Chem.* **1984**, *22*, 847–850.

43 S. Kim, E. M. Pearce, *Polym. Preprints* **1986**, *27*, 97–99.

44 D. Likhatchev, C. Gutierre-Wing, I. Kardash, R. Vera-Graziano, *J. Appl. Polym. Sci.* **1996**, *59*, 725–735.

45 P. Bassignans, C. Cogrossi, M. Gandino, *Spetrochim. Acta.* **1963**, *19*, 1885–1897.